On the Analysis of the Complex Forbush Decreases
of January 2005

**A. Papaioannou · O. Malandraki · A. Belov · R. Skoug ·
H. Mavromichalaki · E. Eroshenko · A. Abunin ·
S. Lepri**

Abstract In this work an analysis of a series of complex cosmic ray events that occurred
between 17 January 2005 and 23 January 2005 using solar, interplanetary and ground based
cosmic ray data is being performed. The investigated period was characterized both by sig-
nificant galactic cosmic ray (GCR) and solar cosmic ray (SCR) variations with highlighted
cases such as the noticeable series of Forbush effects (FEs) from 17 January 2005 to 20 Jan-
uary 2005, the Forbush decrease (FD) on 21 January 2005 and the ground level enhancement
(GLE) of the cosmic ray counter measurements on 20 January 2005. The analysis is focusing

A. Papaioannou (✉) · H. Mavromichalaki
Nuclear and Particle Physics Section, Physics Department, National and Kapodistrian University of
Athens, Zografos, 15771 Athens, Greece
e-mail: atpapaio@phys.uoa.gr

H. Mavromichalaki
e-mail: emavromi@phys.uoa.gr

O. Malandraki
Institute of Astronomy and Astrophysics, National Observatory of Athens, Athens, Greece
e-mail: omaland@astro.noa.gr

A. Belov · E. Eroshenko · A. Abunin
Institute of Terrestrial Magnetism, Ionosphere and Radio Wave Propagation (IZMIRAN) of the Russian
Academy of Sciences, after Pushkov, Moscow Region, Russia

A. Belov
e-mail: abelov@izmiran.ru

E. Eroshenko
e-mail: erosh@izmiran.ru

R. Skoug
Space Science and Applications Group ISR-1, MS D466, Los Alamos National Laboratory, Los
Alamos, USA
e-mail: rskoug@lanl.gov

S. Lepri
The University of Michigan, Ann Arbor, MI 48109, USA
e-mail: slepri@umich.edu

Springer

on the aforementioned FE cases, with special attention drawn on the 21 January 2005, FD event, which demonstrated several exceptional features testifying its uniqueness. Data from the ACE spacecraft, together with GOES X-ray recordings and LASCO CME coronagraph images were used in conjunction to the ground based recordings of the Worldwide Neutron Monitor Network, the interplanetary data of OMNI database and the geomagnetic activity manifestations denoted by K_p and D_{st} indices. More than that, cosmic ray characteristics as density, anisotropy and density gradients were also calculated. The results illustrate the state of the interplanetary space that cosmic rays crossed and their corresponding modulation with respect to the multiple extreme solar events of this period. In addition, the western location of the 21 January 2005 solar source indicates a new cosmic ray feature, which connects the position of the solar source to the cosmic ray anisotropy variations. In the future, this feature could serve as an indicator of the solar source and can prove to be a valuable asset, especially when satellite data are unavailable.

Keywords Cosmic rays · Coronal mass ejections · Forbush decreases · Interplanetary coronal mass ejections · Magnetic clouds

1. Introduction

Forbush decreases (FDs) are observed as transient decreases with relatively fast cosmic ray (CR) intensity depression followed by a slower recovery on the time scale of several days (Forbush, 1958; Lockwood, 1971; Belov, 2008; Cane, 2000). These events are generally interpreted as a result of the influence of coronal mass ejections (CMEs) and/or high-speed streams of the solar wind from the coronal holes on the background cosmic rays. Several theories describe the theoretical background of FDs (Gold, 1959; Parker, 1965; Krymsky *et al.*, 1981; Wibberenz *et al.*, 1998). The registered variations of CR intensity are due to the interplanetary shock waves, to the high-speed solar wind streams and to the magnetic clouds. A number of papers in the field deal with the triggering of FDs and CR variability in general (Lockwood, 1971; Le Roux and Potgieter, 1991; Cane, 2000).

Furthermore, during extreme solar events, as solar flares (SFs) and coronal mass ejections (CMEs), intense solar energetic particles (SEPs) are registered by neutron monitors as ground level enhancements (GLEs). The latter events are sharp and short increases of CR intensity, on the time scale of several hours (Smart and Shea, 2002; El-Borie, 2003).

During the declining phase of solar cycle 23, solar activity was prevalent (see, *e.g.*, Hudson, 2007; Malandraki *et al.*, 2007, 2009) resulting into a number of GLEs and intense FDs. We here examine the evolution of CR intensity during the period of intense solar activity observed in January 2005 and the resulting events, which were registered by neutron monitors (NMs). In particular, January 2005 was characterized by significant galactic cosmic ray (GCR) and solar cosmic ray (SCR) variations (Dorotovič *et al.*, 2008). Time profiles of these variations are presented in Figure 1. Specifically, the most noticeable FDs of this time period began on 17 January 2005, with a series of Forbush effects (FEs) (Belov *et al.*, 2001) subsequently registered, namely: on 17 January at 07:48 UT with an amplitude of 6.6% for GCR with 10 GV rigidity, on 18 January at 06:00 UT (11.8%), on 20 January at 04:00 UT (0.6%) and on 21 January at 18:11 UT (9%). SCR had a leading role on 20 January 2005 when a sudden enhancement in cosmic ray intensity measurements was registered (22%), an event listed as GLE69. Many experts in the field studied this GLE case and produced various well-described results (Belov *et al.*, 2006;
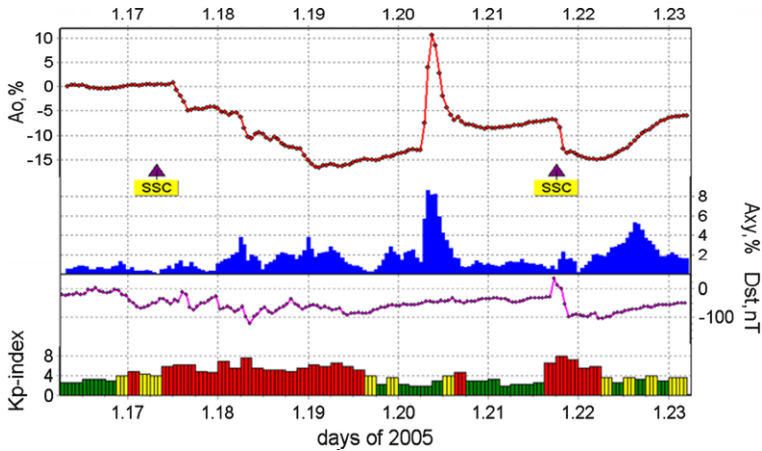
Figure 1 The recorded cosmic ray intensity variations (upper panel) and the corresponding geomagnetic activity (lower panel) from 17 to 23 January 2005.

Plainaki *et al.*, 2007; Vashenyuk *et al.*, 2008; Moraal, Reinecke, and McCracken, 2009; Buetikofer *et al.*, 2007; among many other contributions). The current work is focused on the aforementioned FDs, highlighting the one registered on 21 January 2005, since the interest for this case lies at several features testifying its uniqueness, all of which will be investigated in full extent.

2. Data and Instrumentation

2.1. Data Selection

Parameters used in this particular analysis include cosmic ray density (A_0) and anisotropy (A_{xy}, the equatorial component of the first harmonic of the anisotropy), solar wind data (velocity, temperature and density), IMF magnitude and components as well as solar data and geomagnetic activity indices (K_p and D_{st}). The main tool of the study was the IZMIRAN database on Forbush effects and interplanetary disturbances, which uses as source data the neutron monitor hourly registered values, GOES measurements (continuously updated) and OMNI database (Asipenka *et al.*, 2009). In addition, several websites providing datasets have been used. Namely: http://www.ngdc.noaa.gov, http://omniweb.gsfc.nasa.gov/ow.html, http://sec.ts.astro.it/sec_ui.php, http://www.srl.caltech.edu/ACE/ASC/level2/lvl2DATA_SWEPAM.html, CME data from the SOHO/LASCO CME catalogue compiled by S. Yashiro and G. Michalek (available at: http://cdaw.gsfc.nasa.gov), the list of SSCs from ftp://ftp.ngdc.noaa.gov/STP/SOLAR_DATA/SUDDEN_COMMENCEMENTS/ and solar flares reported in the solar geophysical data http://sgd.ngdc.noaa.gov/sgd/jsp/solarindex.jsp. It should also be added that this database includes neutron monitor data from stations distributed all over the world ($40 - 45$ stations), including the unique properties of each station as coupling coefficients, asymptotic directions and yield functions (Asipenka *et al.*, 2009).

2.2. Calculation Methods

The calculations of CR density (A_0) and the first harmonic of anisotropy (A_{xy}) for 10 GV cosmic rays are being performed through the global survey method (GSM) (Belov *et al.*,

2003, 2005, 2009a; Asipenka *et al.*, 2009). A first step is the simulation of the expected CR intensity at each station, taking into account the special characteristics of the particular neutron monitor (*e.g.* cut-off rigidity, asymptotic directions, altitude) by means of coupling functions and coefficients (Belov *et al.*, 2005). The second step of the calculations includes the fitting of the actual data to the expected simulation. As a result, a set of CR characteristics (as A_0 and A_{xy}) at definite rigidities (R) beyond the magnetosphere are deduced. The usage of GSM results for 10 GV is justified by the fact that this rigidity is close to the effective rigidity of the majority of high and mid-latitude neutron monitors, and CR variations at 10 GV reflect all solar wind disturbances responsible for the FDs (Papaioannou *et al.*, 2009a).

The advantages of GSM usage can be summarized as follows: *i*) hourly averages of A_0 and A_{xy} derived by GSM are global CR characteristics beyond the magnetosphere and do not depend on the local position of detectors and *ii*) A_0 and A_{xy} are obtained with high accuracy ($\approx 0.05\%$ for hourly means) providing more precise estimations of FE parameters.

Furthermore, the spatial distribution of CRs, leading to CR density gradients has been calculated by the convection – diffusion model of anisotropy as introduced by Krymsky (1964) and developed by Belov (1987) and by Chen and Bieber (1993). The implementation of this method is described in detail by Belov *et al.* (1987) and Papaioannou *et al.* (2009b). The basis of the method is the usage of the components of the anisotropy that have been calculated by GSM as an input for the calculation of the three-dimensional density gradient (g_x, g_y, g_z). Through GSM, it has been shown that the diurnal anisotropy (A_{xy}) has a perceptible increase which is proportional to the magnitude of the following FD, directly before the sudden storm commencement (SSC).

3. Solar Activity

The main sunspot group on the Sun during January 2005 was NOAA AR 720, which caused extreme space weather conditions from 14 – 22 January 2005. Its largest event was an X7.1 flare on 20 January. The AR first came into view on 11 January and rapidly grew in size and complexity, although until 13 January, it was responsible for only a few B flares. From 14 January onwards, when the group had grown to its biggest size, AR 720 marked a new period of activity and until its disappearance at the west limb on 23 January, it produced five X-flares, and 17 M-flares. At the same time, AR 718 and AR 719 were also relatively active, each producing two M-flares. Since 14:08 UT of 15 January, the position of AR 720 was at western locations on the Sun; therefore, it provided mostly events of western origin. Some of the most highlighted are indicated.

A long duration M8.6 flare peaked at 06:38 UT (N11E06) of 15 January and was accompanied by a full halo CME at 06:30 UT (Figure 2, upper left panel). A long duration X2.6 flare peaked at 23:02 UT, 15 January. A full halo CME (Figure 2, upper middle panel) with median/maximum speed of 1488/1960 km s^{-1} was detected by CACTus (Robbrecht and Berghamns, 2004) at 23:06 UT in LASCO/C2. It is important to note that time refers to the first appearance of the CME in the C2 coronagraph (> 1.5 solar radii). An X3.8 flare was seen, with an increase in the X-ray radiation output curve before the peak time at 09:52 UT, 17 January. A full halo CME at 1567/1974 km s^{-1} was detected at 09:30 UT (Figure 2, upper right panel) and another one on the same day at 09:54 UT (Figure 2, bottom left panel). A powerful X1.3 flare peaked at 08:22 UT (N11W47), 19 January with an associated full halo CME coming out of the occulting disk of LASCO/C2 at 08:29 with a median/maximum speed of 1516/1977 km s^{-1} (Figure 2, bottom middle panel). The last flare was the most energetic one: it peaked at the value of X7.1 at 07:01 UT (N12W58) on 20 January. A full halo
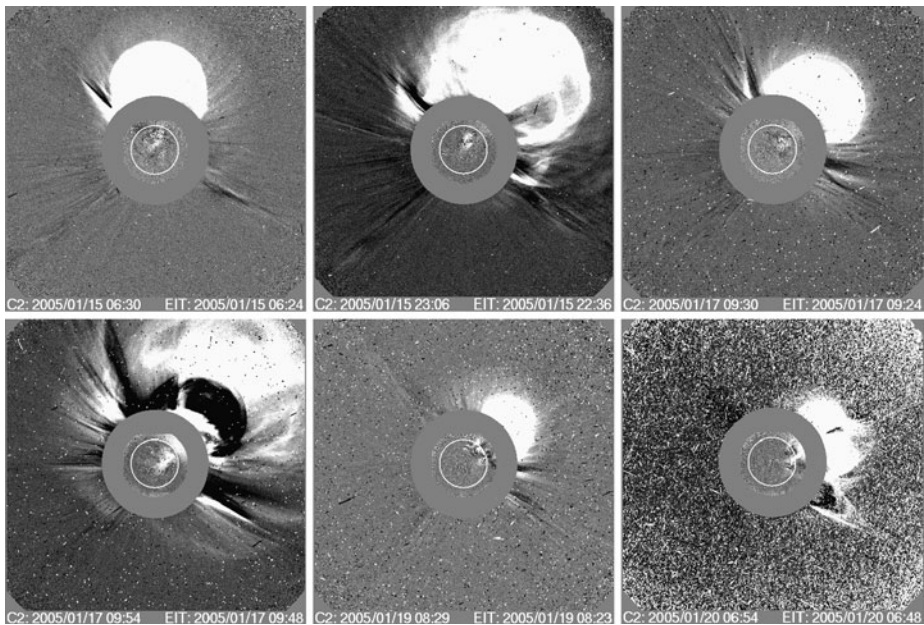
Figure 2 Coronal mass ejections (CMEs) of January 2005 which prevailed in interplanetary space and dominated the GCRs journey resulting into significant FDs.

CME was detected at 06:54 UT (Figure 2, bottom right panel). Gopalswamy *et al.* (2005) have analyzed combined SOHO/LASCO and SOHO/EIT measurements and have obtained a speed of 3242 km s^{-1} for this latter CME.

4. Interplanetary Space

Plasma and magnetic field parameters observed by ACE in the interplanetary medium during the period 16–24 January 2005 are presented in Figure 3. From top to bottom panels it shows color-coded pitch-angle velocity distributions $f(v)$ of 272 eV electrons (cm^{-6} s^3), proton density (cm^{-3}), temperature (K), and speed (km s^{-1}), the alpha to proton ratio, composition data, magnetic field magnitude (nT) and directions (GSE coordinates). Black horizontal bars on top of the figure indicate periods with counter-streaming electrons whereas hatched horizontal bars denote periods with no SWEPAM electron measurements available. In the third panel a comparison of the observed proton temperature (black line) with the expected temperature T_{ex} (red line) appropriate for normally expanding solar wind is shown. The temperature T_{ex} is typically that found in the ambient solar wind as a function of observed speed V_{sw} and is inferred by using an empirical correlation between the proton temperature and the solar wind speed (see, *e.g.*, Neugebauer *et al.*, 2003; Elliott *et al.*, 2005). Such temperature comparisons have been systematically used for ICME identifications (see, *e.g.*, Gosling, Pizzo, and Bame, 1973; Cane and Richardson, 2003). The intervals of reduced resolution proton data are due to the intense fluxes of solar energetic particles. During these periods 64 s data collected approximately every 33 minutes by SWEPAM are shown. This high background level also affects the SWEPAM electron measurements (see, *e.g.*, Skoug *et al.*, 2004). At 07:12 UT on 17 January a forward shock is ob-
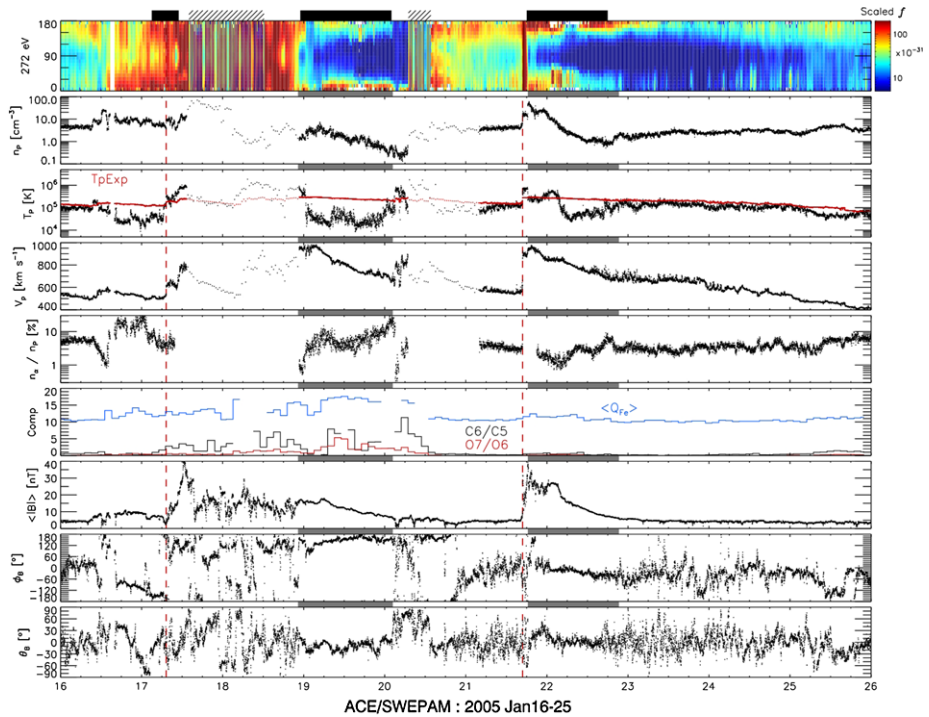
Figure 3 Interplanetary manifestations registered by ACE/SWEPAM, from 16 to 26 January 2005.
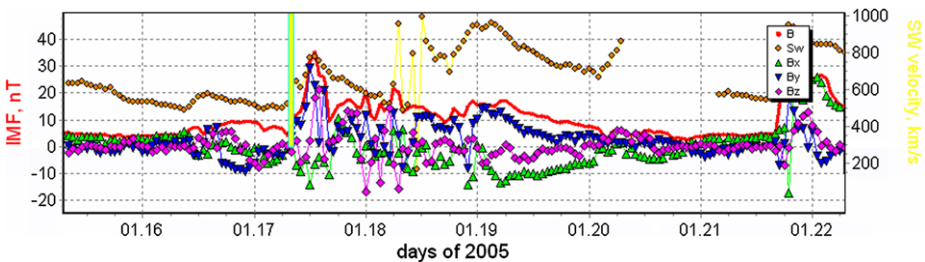
Figure 4 Interplanetary magnetic field (IMF) and solar wind (S_W) measurements from 17 to 23 January 2005 by OMNI database.

served (denoted in Figure 3 by a vertical dashed line). After the passage of this shock an extended period of an ICME sheath is observed with highly variable magnetic field magnitude and directions, and typical for high proton temperatures. Around 23:00 UT, on 17 January, 02:30 UT and 05:30 UT on 18 January several large changes in B and B_z are visible (Figures 3 and 4). Two further days, 18 and 19 January, with severe geomagnetic disturbances were followed. At 22:19 UT on 18 January a significant drop in the magnetic field fluctuation level is observed in association with counter-streaming electrons. The proton temperature also drops abruptly to lower than expected values at about that time, and enhanced alpha particle abundances are observed during this interval. The field azimuth angle shows a smooth and coherent rotation of the magnetic field vector typical of a flux rope. These char-

acteristics indicate that this is a magnetic cloud (MC) (Lepping, Burlaga, and Jones, 1990; Bothmer and Schwenn, 1998). These signatures last until around 02:24 UT on 20 January, which is indicative of the trailing boundary of the MC. This ICME also shows composition signatures, including elevated iron, carbon, and oxygen charge states. Interestingly, elevated iron charge states were also observed prior to this event, in association with an earlier ICME. This extension of high-charge state iron beyond the ICME boundaries is unusual. Grey shaded bars between panels in Figure 3 denote periods with ICME characteristics.

A second ICME was observed near Earth on 21 – 22 January 2005, obviously associated with the high-speed CME at the Sun on 20 January 2005. Based on the magnetic field and plasma *in situ* measurements, Foullon *et al.* (2007) in their multi-spacecraft study have identified the boundaries of this ICME observed at ACE on 21 – 22 January 2005. A forward shock, indicated in Figure 3 by a dotted vertical line, was observed by ACE around 16:47 UT on 21 January. The solar wind speed jumped from 600 to 1000 km s^{-1}. The IMF B_z component increased to more than 20 nT, leading to a sudden severe geomagnetic storm with estimated K_p reaching up to 8 on 21 – 22 January 2005 and D_{st} decreased to -105 nT (Figure 1). A first encounter with the ICME occurred around 18:20 UT on 21 January 2005. This ICME included magnetic cloud signatures from 00:45 UT – 21:20 UT on 22 January 2005. Solar wind charge states during this event showed very weak enhancements, but were generally typical of solar wind distributions.

5. Cosmic Ray Activity

At this point it is important to divide our analysis into two periods of interest, so that it can be more concrete and clear. Therefore, the first period – which will be indicated from this point on as Forbush Decrease case one (FD1) – includes the series of FEs registered from 17 to 20 January 2005, thus focusing on four FEs in very close succession. The second period of interest focuses on the significant FD of 21 January 2005 – which will be referred to as Forbush Decrease case two (FD2).

As can be seen in Figures 1 and 4, all the solar/interplanetary sources of these FDs are geoeffective and in agreement with a number of interplanetary shocks impinging on the Earth's magnetosphere during this period. Due to the complexity of the magnetic field at this time and in relation to low resolution interplanetary data (Figure 4), only two sudden storm commencements (SSC) are clearly registered (Figure 1). The first one appears on the initiation of FD1, while the second one occurs on 21 January 2005, marking the beginning of FD2.

Forbush Decrease Case One (FD1)   A series of FEs registered in very close succession from 17 to 20 January 2005. The onset of this series of events was identified by a SSC on 07:48 UT on 17 January, leading to a decrease of 6.6% for 10 GV cosmic ray particles. From this point on, the exact impact of the various solar sources is rather unclear, mostly due to low resolution solar wind data. What is certain, though, is the complexity of the magnetic field and its accompanied distortion (Figures 2 and 4). In order to provide more accurate explanations of the on-going series of FEs, discrimination was mandatory. The first of the series of FEs is highly likely the offspring of the merging of 15 January 2005 CMEs at 06:30 UT and 23:06 UT (Figure 2). The second one (18 January, 06:00 UT (11.8%)) falls into the period of extensive magnetic field complexity, arising from numerous CMEs on 17 January. This is presumably the reason why another SSC is not clearly indicated. GCRs provide input in this case, though. The anisotropy A_{xy} rose up to $\approx 4\%$ at the exact time of
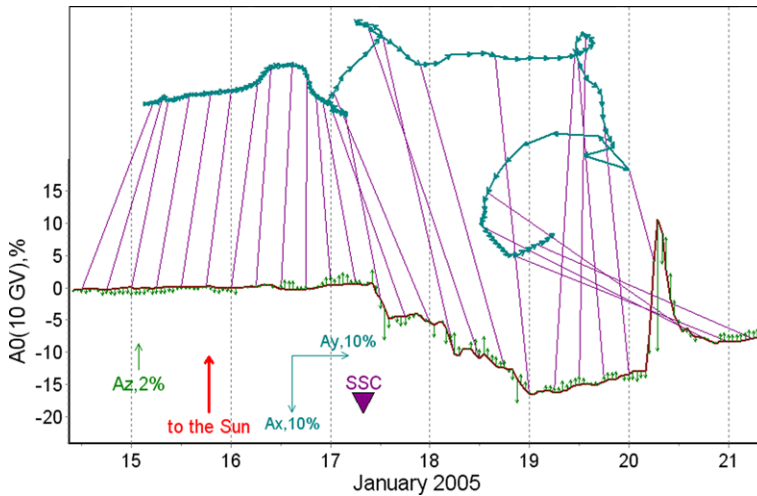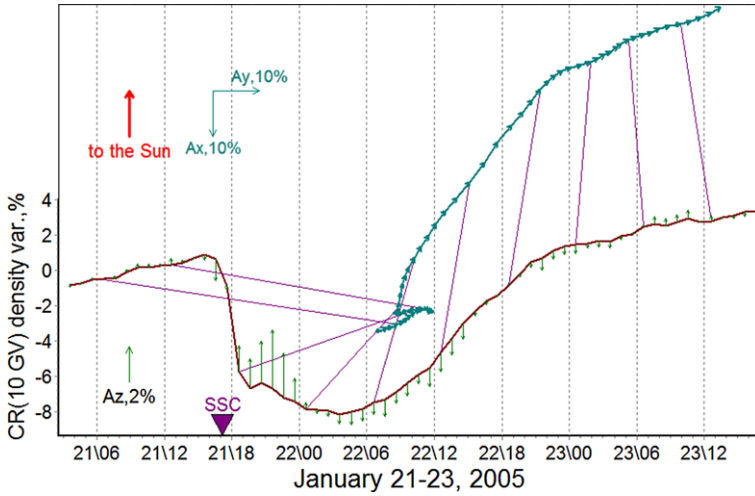
Figure 5 Illustration of CR anisotropy variations (A_{xy} – vector diagram), on CR density (A_0) from 15 to 21 January 2005, focusing on the FD1 case.

FE onset (Figure 1) and, moreover, it changed direction abruptly (Figure 5) – both possible evidence of shock arrival, implying the arrival of a new interplanetary disturbance at this point (Belov *et al.* 2003, 2009b). Moreover, later that day, the influence of the forthcoming MC is indicated in the cosmic ray behavior. While still during the declining phase of the second FE (18 January, 06:00 UT), due to the MC arrival a further drop of $\approx 1\%$ occurred, marked on 22:19 UT (Figure 1).

The last in the series of FEs was registered on 20 January, 04:00 UT (0.6%), but was not clearly seen at all stations due to the solar cosmic rays (SCR) at that time. In order to identify the special features of this latter FE, mid- to low-latitude NM stations (*e.g.* Athens and ESOI NM stations), incapable of registering SCR, have been used. This event could be related to the western CME of the previous day (19 January). It is an actual example of the typical small and short FDs that are produced by western solar sources (Belov, 2008).

Forbush Decrease Case Two (FD2) On 21 January 2005 a SSC was registered at 18:11 UT. As a result a large FD of 9% amplitude for 10 GV cosmic rays was recorded (Figure 1). The geomagnetic indices revealed very disturbed conditions with D_{st} reaching -105 nT and K_p rising up to 8. The interplanetary magnetic field (IMF) was rather strong, 29.5 nT (Figure 4). Although the triggering of FD2 was rather clear and well connected to its solar source, its development is far from regular. As can be seen by Figures 1 and 6, FD2 reached its minimum in a couple of hours – which is proof of a very strongly modulated period – and then entered the recovery phase. This is the most highlighted characteristic of FD2. The recovery phase is not only very gradual, but the A_{xy} component of the anisotropy presents a smooth increasing profile and the anisotropy A_{xy} rose up to 5.26% (Figure 1). The usual case is that the A_{xy} component increases rather sharply at the initial phase of the FD, following a decrement during the decreasing phase, and then rises up again at a lower level from the FD onset, almost until the end of the recovery phase (Belov *et al.*, 2003). For the first time during this unusual FD not only a gradual increase of A_{xy} is being recorded but also the second A_{xy} peak is extensively bigger ($\approx 6\%$) in comparison to the FD onset A_{xy} peak ($\approx 2\%$).

Figure 6 Illustration of CR anisotropy variations (A_{xy} – vector diagram), on CR density (A_0) from 21 to 23 January 2005, focusing on the FD2 case.
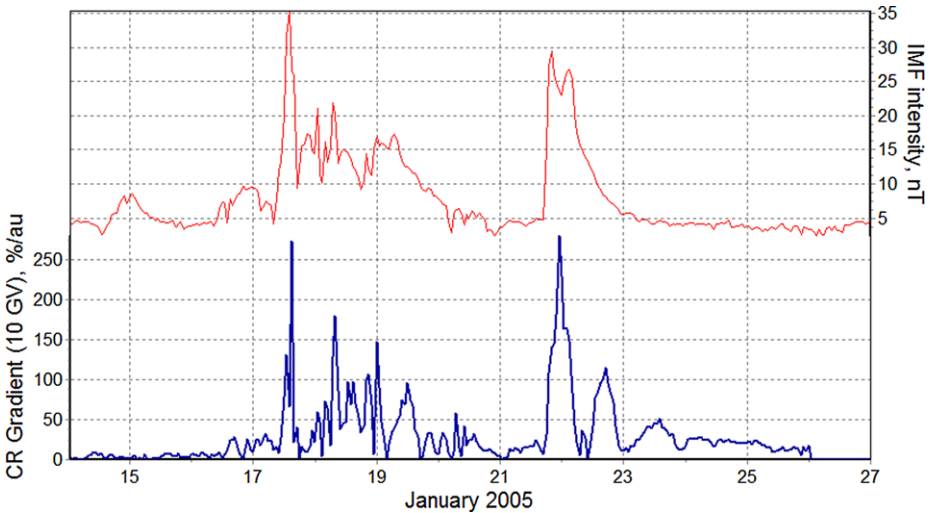
Figure 7 Cosmic ray gradient (g_{xy}) (bottom panel) and IMF intensity deduced by OMNI data (upper panel) from 15 to 26 January 2005.

Cosmic Ray Density Gradients   The calculated gradient of cosmic ray density with respect to IMF measurements is presented in Figure 7. It is clear that in all FE cases gradient peaks are associated with IMF peaks, indicating the presence of a series of FEs during FD1 period and a clear FD of great magnitude at 21 January 2005 (FD2). The result of the calculations for FD1 states a gradient of $\approx 250\%$/AU for 17 January 2005 (FE magnitude 6.6% for 10 GV rigidity cosmic rays), gradient of $\approx 180\%$/AU for 18 January 2005 (FE magnitude 11.8%) and a gradient of $\approx 50\%$/AU for 20 January 2005 (FE magnitude 0.6%). Furthermore, the calculated density gradient for 21 January 2005 case (FD2) reveals a $\approx 250\%$/AU gradient

Figure 8 FD magnitude for all events with registered western source (> 35°, 161 events) in relation to the maximum decrement during the event. The 21 January 2005 case stands out, as it is the sole dot at the right end corner of the figure. It has a decrement of ≈ 5% and a corresponding FD magnitude of 9%.
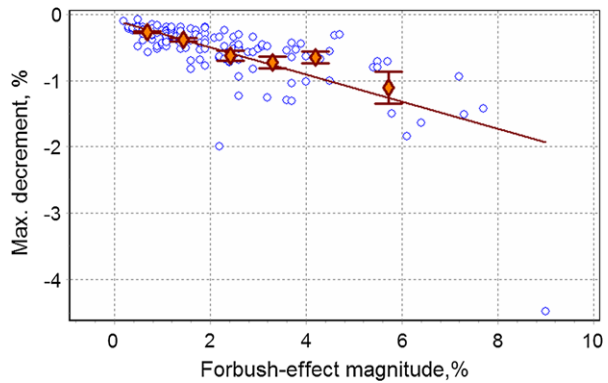
at the initiation of the decrease and a following density gradient of ≈ 100%/AU during the recovery phase.

6. Discussion

Forbush decrease case 1 (FD1) is a very complex phenomenon, due to the interrelation of many intense solar events of this period. The existence of many CMEs at this time resulted in a series of FEs. Usually, such series, especially of western origin, end with a short and small FD, similar to the one on 20 January 2005 for the case under investigation. Moreover, low resolution solar wind data (Figures 2 and 4), at some crucial points of the event development, lead to unclear unfolding of the situation. Nevertheless, there is clear evidence on specific parts of the event. First of all, the onset of the FE of 17 January 2005 (07:48 UT) is coincidental to the SSC, which is the result of the possible merging of halo CMEs of 15 January 2005 (06:30 and 23:06 UT). Due to the large amount of released plasma, which was the output of the CMEs that occurred during this time (on 15 January 2005) in very close succession, it is impossible to clearly identify the shocks that followed. Nevertheless, a possible shock is evident for 18 January 2005 as the GCRs anisotropy reveals. In particular, at that time A_{xy} rose up to ≈ 4% at the exact time of the FE initiation (Figure 1) and more than that it changed its direction in a most abrupt way (Figure 5). Finally, as can be observed at Figure 3, the disturbed sheath region lasted for almost one and a half days before the encounter with the MC. This behavior is abnormal and it is possibly due to the large number of CMEs of this period that caused disorder in the interplanetary magnetic field.

Moreover, it is possible to propose that the series of FEs which constitute the FD1 case did not end with the small FD of 20 January 2005 but continued unexpectedly with FD2. Therefore, both cases (namely FD1 and FD2) can be considered as an extended case of a FD storm.

Attention should be drawn to the exceptional characteristics of FD2 on 21 January 2005. First of all, this was the result of a western CME originating at the same footprint as the solar flare that provided the extreme GLE of the previous day (20 January 2005 – N12W58). Moreover, by checking all FDs ever recorded, induced by western sources (> W35°, 161 events), it is shown that the 21 January 2005 FD constitutes a unique category, which makes it stand out from the rest of the cases (Figure 8). It has the biggest FD magnitude among all the other western induced events (9%, for 10 GV rigidity particles) and its maximum decrement is ≈ 5%, which demonstrates very abrupt changes during the decreasing phase of the FD. Again it is the highest decrement ever recorded for such events (Figure 8).

Furthermore, the calculated anisotropy and the corresponding gradients of this time proved to be far from usual. As shown in Figure 6, the diurnal anisotropy A_{xy} had a rather unusual behavior. This feature of FD2 can be explained through the combination of the convection diffusion approach for cosmic rays and the available experimental data. The simplified mathematical formulation of the convection diffusion model (Krymsky *et al.*, 1981; Belov, 1987) suggests that the anisotropy vector **A** is proportional to the gradient vector **g**:

$$\mathbf{A} = c \cdot \Lambda \cdot \mathbf{g}, \tag{1}$$

where the factor Λ – which corresponds to the matrix of transport paths – depends on the Larmor radius $r : r = \frac{mu_{\perp}}{qB}$ which is inversely proportional to the strength of the total magnetic field B. It seems that in order to justify the anisotropy of any period a balance must be achieved between r and **g**. Taking into account the registered IMF and the gradient of this period (Figures 2 and 4), one might be led to the following conclusion: at the onset of the FD (21 January 2005, 18:11 UT) IMF was at high levels (30 nT) – leading to a small Λ –, and the two dimensional gradient (g_{xy}) was also rather big ($\approx 260\%/AU$) (Figure 7), leading to an enhanced A_{xy} parameter of $\approx 2\%$. At the end of the event the IMF is ≈ 6 nT – small and thus leading to a big Λ factor –, while g_{xy} is $\approx 100\%/AU$ (Figure 7), resulting after Equation (1) at an A_{xy} value of $\approx 6\%$. A closer look at the data reveals more details. Density gradients have a typical behavior: at the onset of the FD, g_{xy} is usually larger compared to the one calculated for the end of the FD. This is actually evident in the case of FD2, where the density gradients vary from the onset of the FD to its ending phase by a factor of approximately 2.3. This is an expected feature. Thus, the existence of a very large CR gradient, not only at the beginning of the event but also during the recovering phase, together with IMF intensity is the main reason for the unusual A_{xy} values.

7. Conclusions

From the above analysis of the events of January 2005, it is pointed out that the series of FDs which started on 17 January and ended on 23 January (including FD1 and FD2) stands out as a unique example of extended geomagnetic disturbances due to a large number of solar sources and their corresponding registered impact on cosmic rays.

The resulted impact of the aforementioned activity is outlined by the unique case of the 21 January 2005 FD (FD2). In particular we have the following.

i) It seems that it had a strong western CME solar source, associated to an intense SF, both of which produced one of the most effective acceleration of charged particles on the Sun in the history of observations, leading to GLE69. It is a bright example of relations between the accelerating and modulating abilities of solar events (Belov *et al.*, 2009b).

ii) It had the biggest FD magnitude among all the other western induced events (9%, for 10 GV rigidity particles).

iii) It had the maximum decrement ever recorded for western events ($\approx 5\%$).

iv) The diurnal anisotropy A_{xy} of the FD presented unique characteristics. It was rather moderate at the initiation of the event ($\approx 2\%$) and it grew towards the end of the event ($\approx 6\%$).

The most interesting result is the diurnal anisotropy (A_{xy}) observed during this time period. It may be proposed that the increase of A_{xy} is connected to the western solar source of the FD. This is not the first time that a FD of western origin marks an enhancement on A_{xy}.

The case of July 2005 (Papaioannou *et al.*, 2009b), although different in many aspects from the one under investigation in this work, had two common features: *i*) a far western source and *ii*) A_{xy} rose up to 5%. Considering the fact that the FDs of western origin constitute only a small fraction of all FE cases (161 events out of ≈ 800 well identified FEs for the last 50 years), while at the same time only a dozen of them presented extensive magnitude ($> 6\%$) (Figure 8) and that a common registered behavior appeared at two out of these twelve cases (January and July 2005), we have motivation for a further analysis on this kind of events, with the scope to solidly establish the aforementioned result of the connectivity of a western solar source to diurnal GCR anisotropy enhancements. In the future, this could serve as an indicator of solar sources and can prove to be a valuable asset, especially when satellite data are unavailable.

References

Asipenka, A., Belov, A., Eroshenko, E., Klepach, E., Oleneva, V., Yanke, V.: 2009, *Adv. Space Res.* **43**, 708.

Belov, A.: 1987, *Proc. 20th Int. Cosmic Ray Conf.* **4**, 119.

Belov, A.: 2008, In: Gopalswamy, N., Webb, D.F. (eds.) *Universal Heliophysical Processes*, *IAU Symp.* **257**, 439.

Belov, A., Dorman, L., Eroshenko, E., Oleneva, V.: 1987, *Proc. 20th Int. Cosmic Ray Conf.* **4**, 137.

Belov, A., Eroshenko, E., Oleneva, V., Struminsky, A., Yanke, V.: 2001, *Adv. Space Res.* **27**, 625.

Belov, A., Bieber, J., Eroshenko, E., Evenson, P., Pyle, R., Yanke, V.: 2003, *Adv. Space Res.* **31**, 919.

Belov, A., Baisultanova, L., Eroshenko, E., Mavromichalaki, H., Yanke, V., Pchelkin, V., Plainaki, C., Mariatos, G.: 2005, *J. Geophys. Res.* **110**, A09S20.

Belov, A., Eroshenko, E., Mavromichalaki, H., Plainaki, C., Yanke, V.: 2006, *Proc. 29th Int. Cosmic Ray Conf.* **1**, 189.

Belov, A., Asipenka, A., Dryn, E., Eroshenko, E., Kryakunova, O., Oleneva, V., Yanke, V.: 2009a, *Bull. Russ. Acad. Sci.* **73**, 331.

Belov, A., Eroshenko, E., Oleneva, V., Yanke, V.: 2009b, *Proc. 31th Int. Cocmic Ray Conf.* http://icrc2009.uni.lodz.pl/proc/pdf/icrc1004.pdf.

Bothmer, V., Schwenn, R.: 1998, *Ann. Geophys* **16**, 1.

Buetikofer, R., Flueckiger, E., Desorgher, L., Moser, M., Pirard, B.: 2007, In: Mavromichalaki, H., Papaioannou, A. (eds.) *Solar Extreme Events 2007, Fundamental Science and Applied Aspects*, National and Kapodistrian University of Athens, 71.

Cane, H.V.: 2000, *Space Sci. Rev.* **93**, 55.

Cane, H.V., Richardson, I.G.: 2003, *J. Geophys. Res.* **108**, 1156.

Chen, J., Bieber, J.: 1993, *Astrophys. J.* **405**, 375.

Dorotovič, I., Kudela, K., Lorenc, M., Rybansky, K.: 2008, *Solar Phys.* **250**, 339.

Elliott, H.A., McComas, D.J., Schwadron, N.A., Gosling, J.T., Skoug, R.M., Gloeckler, G., Zurbuchen, T.H.: 2005, *J. Geophys. Res.* **110**, A04103.

El-Borie, M.A.: 2003, *Astropart. Phys.* **19**, 549.

Forbush, S.E.: 1958, *J. Geophys. Res.* **63**, 651.

Foullon, C., Owen, C.J., Dasso, S., Green, L.M., Dandouras, I., Elliott, H.A., Fazakerley, A.N., Bogdanova, Y.V., Crooker, N.U.: 2007, *Solar Phys.* **244**, 139.

Gold, T.: 1959, *J. Geophys. Res.* **64**, 1665.

Gosling, J.T., Pizzo, V., Bame, S.J.: 1973, *J. Geophys. Res.* **78**, 2001.

Gopalswamy, N., Xie, H., Yashiro, S., Usoskin, I.: 2005, *Proc. 29th Int. Cosmic Ray Conf.* **1**, 169.

Hudson, H.: 2007, *Astrophys. J. Lett.* **663**, 45.

Krymsky, G.: 1964, *Geomagn. Aeron.* **4**, 977.

Krymsky, G.F., Kuzmin, A.I., Krivoshapkin, P.A., Samsonov, I.S., Skripin, G.V., Transkii, I.A., Chirkov, N.P.: 1981, *Cosmic Rays and Solar Wind*, Nauka, Novosibirsk, 1981 (in Russian).

Lepping, R.P., Burlaga, L.F., Jones, J.A.: 1990, *J. Geophys. Res.* **95**, 11957.

Le Roux, J., Potgieter, M.: 1991, *Astron. Astrophys.* **243**, 531.

Lockwood, J.A.: 1971, *Space Sci. Rev.* **12**, 658.

Malandraki, O.E., Marsden, R.G., Tranquille, C., Forsyth, R.J., Elliott, H.A., Lanzerotti, L.J., Geranios, A.: 2007, *J. Geophys. Res.* **112**, A06111.

Malandraki, O.E., Marsden, R.G., Lario, D., Tranquille, C., Heber, B., Mewaldt, R.A., *et al.*: 2009, *Astrophys. J.* **704**, 469.

Moraal, H., Reinecke, J., McCracken, K.: 2009, *Proc. 31th Int. Cosmic Ray Conf.*, http://icrc2009.uni.lodz. pl/proc/pdf/icrc1553.pdf.

Neugebauer, M., Steinberg, J.T., Tokar, R.L., Barraclough, B.L., Dors, E.E., Wiens, R.C., Gingerich, D.E., Luckey, D., Whiteaker, D.B.: 2003, *Space Sci. Rev.* **105**, 661.

Papaioannou, A., Mavromichalaki, H., Eroshenko, E., Belov, A., Oleneva, V.: 2009a, *Ann. Geophys.* **27**, 1.

Papaioannou, A., Belov, A., Mavromichalaki, H., Eroshenko, E.: 2009b, *Adv. Space Res.* **43**, 582.

Parker, E.: 1965, *Planet. Space Res.* **13**, 9.

Plainaki, C., Belov, A., Eroshenko, E., Mavromichalaki, H., Yanke, V.: 2007, *J. Geophys. Res.* **112**, A04102.

Robbrecht, E., Berghamns, D.: 2004, *Astron. Astrophys.* **425**, 1097.

Skoug, R.H., Gosling, J.T., Steinberg, J.T., McComas, D.J., Smith, C.W., Ness, N.F., Hu, Q., Burlaga, L.F.: 2004, *J. Geophys. Res.* **109**, A9.

Smart, D., Shea, P.: 2002, *Adv. Space Res.* **30**, 1033.

Vashenyuk, E., Miroshnichenko, L., Balabin, Y., Perez-Peraza, J., Gallegos-Lruz, A.: 2008, *Proc. 30th Int. Cosmic Ray Conf.* **1**, 249.

Wibberenz, G., Le Roux, J., Potgieter, M., Bieber, J.: 1998, *Space Sci. Rev.* **83**, 309.